JGR Atmospheres

RESEARCH ARTICLE
10.1029/2022JD036586

Enhanced Deposition of Atmospheric Soluble Iron by Intrusions of Marine Air Masses to East Antarctica

V. H. L. Winton[1,2], **A. R. Bowie**[3,4], **M. A. Curran**[3,5], **and A. D. Moy**[3,5]

[1]Physics and Astronomy, Curtin University, Perth, WA, Australia, [2]Now at Antarctic Research Centre, Victoria University of Wellington, Wellington, New Zealand, [3]Antarctic Climate and Ecosystems Cooperative Research Centre, University of Tasmania, Hobart, TAS, Australia, [4]Institute of Antarctic and Southern Ocean Studies, University of Tasmania, Hobart, TAS, Australia, [5]Australian Antarctic Division, Hobart, TAS, Australia

Key Points:

- Extremely low concentrations of dissolved atmospheric iron are observed in a 10-year snow record from Aurora Basin North (ABN), East Antarctica
- Dissolved iron (dFe) concentrations are enhanced in synoptic warm air masses
- The highest dFe concentrations at ABN reflect atmospheric transport and processing rather than source signals (dust or biomass burning)

Supporting Information:

Supporting Information may be found in the online version of this article.

Correspondence to:

V. H. L. Winton,
holly.winton@vuw.ac.nz

Citation:

Winton, V. H. L., Bowie, A. R., Curran, M. A., & Moy, A. D. (2022). Enhanced deposition of atmospheric soluble iron by intrusions of marine air masses to East Antarctica. *Journal of Geophysical Research: Atmospheres*, *127*, e2022JD036586. https://doi.org/10.1029/2022JD036586

Received 31 JAN 2022
Accepted 16 JUN 2022

Author Contributions:

Conceptualization: V. H. L. Winton
Data curation: V. H. L. Winton, M. A. Curran
Formal analysis: V. H. L. Winton
Funding acquisition: V. H. L. Winton, M. A. Curran
Investigation: V. H. L. Winton, M. A. Curran
Methodology: V. H. L. Winton
Project Administration: V. H. L. Winton, M. A. Curran
Resources: M. A. Curran
Supervision: A. R. Bowie
Validation: V. H. L. Winton

Abstract Bio-essential iron can relieve nutrient limitation and stimulate marine productivity in the Southern Ocean. The fractional iron solubility of aerosol iron is an important variable determining iron availability for biological uptake. However, estimates of dissolved iron (dFe; iron < 0.2 μm) and the factors driving the variability of fractional iron solubility in pristine air masses are largely unquantified. To constrain inputs of fractional iron solubility to remote East Antarctic waters, dFe, total dissolvable iron (TDFe), trace elements and refractory black carbon were analyzed in a 9-year-old snow pit (2005–2014) from a new ice core site at Aurora Basin North (ABN) in Wilkes Land, East Antarctica. Extremely low annual dFe deposition fluxes were estimated (0.2×10^{-6} g m^{-2} y^{-1}), while annual TDFe deposition fluxes (70×10^{-6} g m^{-2} y^{-1}) were comparable to other Antarctic sites. TDFe is dominantly sourced from mineral dust. Unlike coastal Antarctic sites where the variability of fractional iron solubility in modern snow is explained by a mixture of dust and biomass burning sources, dFe deposition and fractional iron solubility at ABN (ranging between 0.1% and 6%) is enhanced in episodic high precipitation events from synoptic warm air masses. Enhanced fractional iron solubility reaching the high elevation site at ABN is suggested through the mechanism of cloud processing of background mineral dust that modifies the dust chemistry and increases iron dissolution during long-range transport. This study highlights a complex interplay of sources and processes that drive fractional iron solubility in pristine air masses.

Plain Language Summary Photosynthetic microorganisms in the Southern Ocean play a critical role in the global carbon cycle and support the extensive biodiversity and food web of the ocean. These organisms are responsible for a process called primary productivity which converts carbon dioxide into organic molecules via photosynthesis. Atmospheric deposition of iron to the ocean is an essential nutrient for primary production in the Southern Ocean. Without iron supply, primary production is limited. While iron is highly abundant on Earth, it is also very insoluble in seawater, making every source of soluble iron critical to life in the ocean. Soluble iron is an important variable determining iron availability for biological uptake. This study quantifies atmospheric deposition of soluble iron to Aurora Basin North, a new ice core site in East Antarctica. We find that soluble iron is enhanced in large snowfall events due to dust processing by clouds in the atmosphere that make it more soluble.

1. Introduction

Primary production is limited by micronutrient iron (Fe) in the high nutrient low chlorophyll (HNLC) modern Southern Ocean (e.g., P. W. Boyd et al., 2000). With global climate change effects predicted to be particularly severe in the Southern Ocean, phytoplankton will be influenced by many oceanic stressors, including iron supply (P. W. Boyd et al., 2015, 2019; Deppeler & Davidson, 2017; Henley et al., 2020; Morley et al., 2020; Pinkerton et al., 2021; Rose et al., 2009; Tagliabue et al., 2017). Therefore, quantifying the bioavailability and understanding the factors that drive the solubility of iron inputs to Southern Ocean surface waters is crucial to understand how iron biogeochemical cycles and the biological pump will respond to a changing ocean.

On a global scale, atmospheric iron has received much attention in terms of the factors that drive its solubility. Stepwise leaching experiments of fractional iron solubility in atmospheric samples are used as an approximation of the bioavailable fraction of iron supplied to ocean surface waters (Mahowald et al., 2018). Soluble or dissolved iron (dFe) in these experiments is operationally defined as the iron passing through a 0.2 or 0.45 μm

Visualization: V. H. L. Winton
Writing – original draft: V. H. L. Winton
Writing – review & editing: V. H. L. Winton, A. R. Bowie, M. A. Curran, A. D. Moy

filter. The large variability of dFe in the atmosphere has been attributed to a mixture of sources (i.e., mineral dust vs. combustion sources (Sholkovitz et al., 2012)) and atmospheric processes that increase the solubility of iron during aerosol aging and atmospheric transport. Such atmospheric processes include cloud processing, organic complexation, photochemical reactions, and the interaction of iron bearing mineral dust with air masses laden with polluted, acidic or combustion derived aerosol (e.g., Y. Chen & Siefert, 2004; Hand et al., 2004; Ito & Shi, 2015; W. Li et al., 2017; Miller et al., 1995; Paris et al., 2011; Shi et al., 2015].

Marine microorganisms in most of the world's oceans depend on atmospheric iron inputs to support their growth, and community structure, thus impacting on marine biogeochemical cycles (Mahowald et al., 2018). In the Southern Ocean the link between atmospheric iron inputs and biological production and carbon export is well recognized (Tagliabue et al., 2017). Atmospheric iron is amongst the sources of new iron to the Southern Ocean, that is, icebergs and ice shelves, upwelling of deep waters, transport from continental margins by ocean currents, and deposition of local and remote mineral dust (Dinniman et al., 2020; Gao et al., 2020; Rivaro et al., 2020; Salmon et al., 2020; Weber, 2020; Winton, Dunbar, et al., 2016). In addition, dFe is entrained from seawater into sea ice during freezing cycles and released in spring (Duprat et al., 2020; Lannuzel et al., 2016). Yet, the Southern Ocean remains relatively under sampled and complex factors are emerging that concern the interplay of sources and atmospheric processing that effect the solubility of atmospheric iron in pristine air masses (Chance et al., 2015; Gao et al., 2013, 2020; Ito et al., 2019; Winton et al., 2015). A factor limiting the number of observations of atmospheric iron over the Southern Ocean is the extremely low concentrations of atmospheric dFe in pristine air masses making trace metal sampling and mitigation of local contamination challenging (Ayers, 2001; Heimburger, Losno, & Triquet, 2013).

Atmosphere dFe deposition over the Southern Ocean has been investigated in relation to three sampling platforms that determine the atmospheric iron deposition regime. The first deposition regime is dry deposition of aerosol iron from land-based (Gao et al., 2020; Heimburger et al., 2012; Heimburger, Losno, Triquet, et al., 2013; Winton et al., 2015) and ship-based (Bowie et al., 2009; Gao et al., 2013) sampling campaigns using high-volume air sampling onto a filter. The temporal resolution of aerosol sampling studies in the Southern Ocean typically ranges from daily to monthly. The second deposition regime is wet deposition of atmospheric iron at land based stations using trace metal clean rain gauges with a hourly temporal resolution (Chance et al., 2015; Heimburger, Losno, & Triquet, 2013). The final is total deposition (wet and dry) in Antarctic snow and ice layers that archive atmospheric dFe over time (Du et al., 2019; Du et al., 2020; Edwards & Sedwick, 2001; K. Liu et al., 2021, 2019; Winton et al., 2014; Winton, Edwards, Delmonte, et al., 2016). The temporal resolution of Antarctic snow pit samples is sub-annual to annual depending on the snow accumulation rate. While standardised leaching methods of fractional iron solubility in aerosols have been proposed (Perron et al., 2020), estimates of fractional iron solubility in Antarctic snow and ice employ a range of leaching protocols. Conway et al. (2015) demonstrated that both acid leachable iron methods (Gaspari et al., 2006; Vallelonga et al., 2013), to constrain the dFe and total dissolvable iron (TDFe) content (unfiltered, weak acid leachable iron) (Du et al., 2019, 2020; Edwards et al., 2006; K. Liu et al., 2019; Winton, Edwards, Delmonte, et al., 2016), can underestimate the total iron fraction in snow and ice, that is, iron contained within the lattice of highly refractory aluminosilicate particles. However, most of the iron contained within Antarctic snow and ice is rendered soluble under mildly acidic conditions (Edwards & Sedwick, 2001). As refractory iron has a low bioavailability for phytoplankton, TDFe concentrations are presented in Antarctic snow and ice studies.

Variations of fractional iron solubility in modern Antarctic snow over time and space have been attributed to a variety of sources. At modern Antarctic snow sites sampled for dFe, the contribution of dFe from mineral dust is attributed to multiple dust provenances from local and/or remote sources. Across Antarctica, remotely sourced mineral dust is considered the background atmospheric dFe source (Du et al., 2019, 2020; Winton, Edwards, Delmonte, et al., 2016). In terms of coastal sites, local mineral dust is an important contributor of dFe in snow as observed at coastal East Antarctica (Gao et al., 2013; K. Liu et al., 2019) and Roosevelt Island (Winton, Edwards, Delmonte, et al., 2016) with McMurdo Sound being the dustiest location in Antarctica (Winton et al., 2014). Biomass burning is an additional dFe source to the Southern Ocean (Tang et al., 2021) and Antarctic coastal snow (Winton, Edwards, Delmonte, et al., 2016). In terms of the variations in dFe sources over the past few decades, mineral dust is also considered as the background dFe source with additional sporadic sources from biomass burning and volcanic emissions in which volcanic derived acidic sulfate can increase dFe in volcanic plumes (Du et al., 2020). However, less attention has been given to atmospheric processing of dFe. dFe deposition

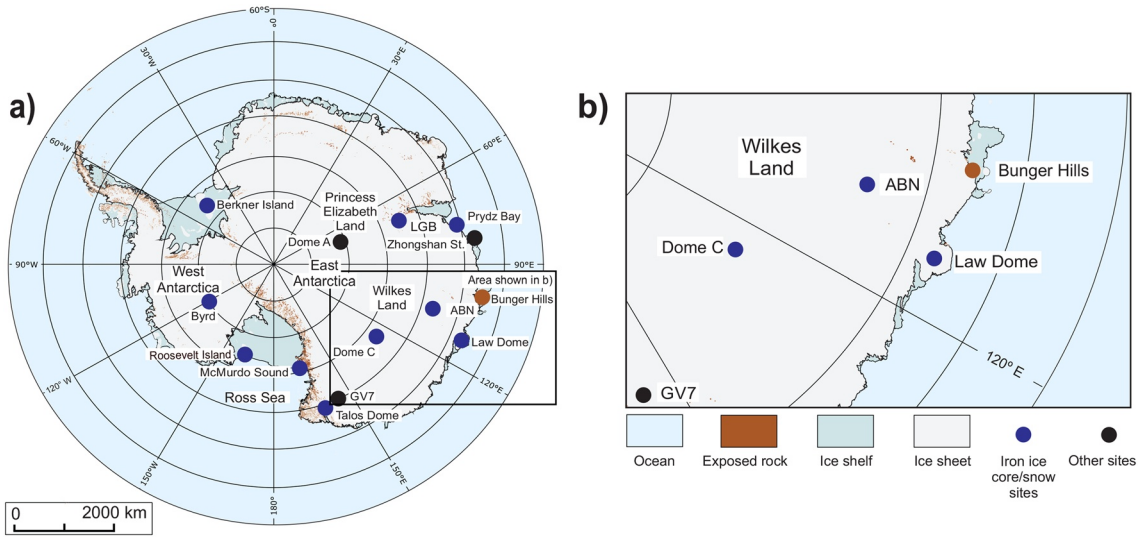

Figure 1. (a) Map of Antarctica showing Antarctic sites where measurements of dissolved iron (dFe) have been made in snow and ice cores, and potential source areas of Antarctic dust. (b) Insert of Wilkes Land highlighting the location of the Aurora Basin North (ABN) study site.

fluxes along a transect from Zhongshan Station to Dome A in East Antarctica peaked around 500 km inland from the coast, and were attributed to different sources and transport processes although the processes are yet to be identified and explained (Du et al., 2019).

To date, studies of dFe in Antarctic snow attribute the variability of fractional iron solubility to a range of sources without much consideration of atmospheric processes. Within the framework of the Aurora Basin North (ABN) ice coring project, which recovered a continuous 303 m long ice core from Wilkes Land, East Antarctica during the 2013/2014 austral Antarctic field season, we show that atmospheric transport and processing can significantly elevate modern dFe concentrations in Antarctic snow.

2. Materials and Methods

2.1. Snow Pit Sampling and Dating

Snow pit samples were collected from ABN, East Antarctica (71° 10.003′S, 110° 22.401′E; 2690 m above sea level, a.s.l.; Figure 1) between 7 and 11 January 2014 during the 2013/2014 ABN ice coring campaign. ABN, located ∼550 km inland from the coast, is an "intermediate" ice core site in terms of its elevation and snow accumulation rate (∼17 cm yr^{-1} water equivalent; w. e.) as it lies between high accumulation coastal sites and low accumulation plateau sites. The predominant wind direction at the site is northwest with a mean wind direction of 279° between 2014 and 2017 (ABN Automatic Weather Station; AWS; 71° 9′59″S, 111° 22′13″E, elevation 2714 m a.s.l.; http://aws.cdaso.cloud.edu.au/ last accessed 15 December 2021). To prevent contamination by camp activities, a designated snow sampling site was located ∼200 m upwind from the ABN ice core drilling camp. Concurrent snow samples were collected from 10 parallel profiles in a 2.5 m deep snow pit for a range of chemical analyses in various laboratories. This study utilizes measurements from three of those profiles which are (a) stable water isotopes ($\delta^{18}O$) and sulfate (SO_4^{2-}) concentrations, (b) black carbon concentrations, and (c) trace elements. Stable water isotopes and SO_4^{2-} concentrations sampled at 2.5 cm resolution, have previously been reported by Servettaz et al. (2020) and are also used in this study. Sulfate and $\delta^{18}O$ were measured in the same profile sample and are referred to as the Australian Antarctic Division (AAD) snow pit in Servettaz et al. (2020). Here we report concentrations of dFe, total dissolvable trace elements (sulfur; S, sodium; Na, titanium; Ti, aluminum; Al, Fe, and lead; Pb) and refractory black carbon (rBC) from two additional profiles sampled at 3 cm resolution.

The snow pit profiles presented here were dated using annual layer counting of a range of trace elements and soluble ions including non-sea-salt total dissolvable sulfur (nss-TDS), non-sea-salt sulfate (nss-SO_4^{2-}) concentrations and $\delta^{18}O$ values. In this study, the dating of the AAD snow pit profile reported in Servettaz et al. (2020) is revised

based on new nss-SO_4^{2-} aerosol timeseries data from nearby Dome C that shows monthly mean nss-SO_4^{2-} aerosol concentrations peak in summer (Becagli et al., 2022). Following the same approach as Servettaz et al. (2020) but using summer rather than spring as the annual marker position for nss-SO_4^{2-} concentration peaks, dating was performed as follows. Summers were determined as 1 January and were positioned where the nss-SO_4^{2-} concentration peak aligned with peaks or shoulders of peaks in the $\delta^{18}O$ record. Due to the high surface roughness at the site and consequent uneven annual snow layers as indicated by the back lit stratigraphy of the snow pit (Figure S1 in Supporting Information S1), spatial variability was observed in the depth profiles of nss-TDS concentrations, nss-SO_4^{2-}concentrations and $\delta^{18}O$ values between parallel profiles. Therefore, nss-TDS peaks were aligned with previously dated summer nss-SO_4^{2-} peaks from Servettaz et al. (2020). Annual layer counting shows the snow pit spans a 9-year period from January 2005 to 2014, with an age uncertainty of ±1 year at the base of the snow pit (Figure S2 in Supporting Information S1). The snow accumulation rate of the snow pit ranged between 3 and 18 cm yr^{-1} (water equivalent; w. e.).

2.2. Trace Element Concentrations, Enrichment Factors and Refractory Black Carbon Concentrations

A detailed description of the snow sampling procedure and analysis of rBC and trace elements at the TRACE Facility, Curtin University can be found in Winton, Edwards, Delmonte, et al. (2016). Briefly, dissolved trace metal fractions were determined by filtering a 10 mL aliquot of snow melt through a 0.2 µm filter. The remaining (unfiltered) sample was leached with 1% HCl (ultrapure) for 3 months to determine the total dissolvable trace element fraction. The leaching time of 3 months was conducted following Edwards & Sedwick (2001) that demonstrated a significant increase in measured iron concentrations of acidified Antarctic snowmelt for up to 3 months following acidification. Total dissolvable solutions and dissolved leachates were analyzed by high-resolution inductively coupled plasma mass spectrometry (HR-ICP-MS). The accuracy of the trace element concentrations was determined by repeated measurements of a certified reference material (ICP200.7-6 solution A, High-Purity Standards, $n = 10$) and resulted in an accuracy of >95% for lead, iron, and aluminum concentrations. HR-ICP-MS operating conditions and analytical figures of merit (including blanks and precision) are reported in Tables S1 and S2 respectively. Due to the low snow density at the surface of the pit and thus low sample volumes, the top 9 cm of the pit contains missing total dissolvable trace element data. Fractional iron solubility was calculated using Equation 1:

$$\text{Fractional iron solubility (\%)} = \frac{\text{dFe}}{\text{TDFe}}\, x\, 100 \tag{1}$$

where dFe is the soluble or dissolved Fe fraction and TDFe is the total dissolvable fraction.

Crustal enrichment factors (EFs) were calculated using the measured total dissolvable trace metal concentrations and Wedepohl (1995) composition of the upper continental crust (UCC) to determine the contribution of mineral dust to the observed total elemental concentrations. We acknowledge the limitation of using UCC values (Eichler et al., 2015; Reimann & Caritat, 2000) as they are not necessarily representative of the ABN site or regional background potential source area (PSA) of dust. Total dissolvable titanium (TDTi) was used as a marker for mineral dust. For an element (Z) in a sample, the EF relative to TDTi is calculated using Equation 2:

$$\text{EF} = \left(\frac{Z}{Ti}\right)_{\text{sample}} \left(\frac{Z}{Ti}\right)_{\text{crust}} \tag{2}$$

rBC was determined using a single particle intracavity laser-induced incandescence photometer (SP2) following Sterle et al. (2013) and Winton, Edwards, Delmonte, et al. (2016). In this study, rBC blank concentrations and detection limits are 0.001 and 0.003 ng g^{-1} respectively. Refractory black carbon and trace element data are available in Winton et al. (2022).

2.3. Stable Water Isotopes and Sulfate Concentrations

Stable water isotopes ($\delta^{18}O$) were measured using a Picarro L2130-i cavity ring down spectrometer at the AAD and the data are reported in Servettaz et al. (2020). The standard deviation for repeated measurements of laboratory reference water samples was less than 0.05 ‰ for $\delta^{18}O$. Sulfate concentrations, reported in Servettaz et al. (2020), were measured at the AAD using a Dionex ion chromatograph according to the methods of Curran

& Palmer (2001) and Plummer et al. (2012). The analytical figures of merit for sulfate include a limit of detection of 0.004 μM, procedural blank concentrations of $P > 0.1$, an accuracy of >97%, and precision of <3%.

3. Results and Discussion

3.1. Refractory Black Carbon

Based on the annual layer counting where nss-TDS defines summer deposition, the deposition of rBC in the ABN snow pit occurs in late winter/spring with additional summer inputs in some years (Figure 2a). The late winter/spring deposition is consistent with the timing of rBC deposition in West Antarctica (Bisiaux et al., 2012), whereas summer rBC deposition is consistent with the timing of rBC deposition at Roosevelt Island, eastern Ross Sea and occasional spikes at GV7, eastern Wilkes Land (Caiazzo et al., 2017). Deposition timing of rBC at ABN is also consistent with atmospheric measurements of rBC at Halley and Neumayer Stations which show a clear seasonal cycle with an autumn/winter minimum and summer maximum (Bodhaine, 1995; Wolff & Cachier, 1998). Exceptionally high rBC concentrations were observed during the 2011/2012 summer in snow pits at Roosevelt Island (Winton, Edwards, Delmonte, et al., 2016) and GV7 (Caiazzo et al., 2017) in which the later study attributed the high rBC concentrations to significantly stronger Australian biomass burning that year. This large rBC event was not observed at ABN suggesting ABN received rBC from a different source that year. rBC concentrations were highest (up to 230 pg g^{-1}) in the top three samples (2013/2014 summer). Concentrations on this order have been observed previously in Antarctic snow and could be due to an exceptionally large burning event that year. However, mean monthly black carbon emissions from five global fire emissions inventories (T. Liu et al., 2020) show that emissions from the 2014 fire season (austral dry winter/spring and spring/summer) were below average that year for the Southern Hemisphere fire regions (Australia-NZ, Southern Hemisphere Africa and Southern Hemisphere South America (FIRECAM; https://globalfires.earthengine.app/view/firecam; last accessed 23 June 2020). Alternatively, the large rBC concentrations may result from contamination from camp activities despite sampling in a designated clean zone upwind of the camp. A few days before snow sampling, issues with the kerosene heater operating at high elevation caused an explosion of soot within a >10 m radius of the camp. Airmass back trajectories show that the wind direction came from the northeast during the "heater explosion event," that is, the predominate wind direction changed and snow pit site was not directly upwind from the camp at this time (Figure S3 in Supporting Information S1). Therefore, the kerosene heater may have contaminated the upper three rBC and trace element samples (~9 cm of snow) in the snow pit. Excluding these surface samples, rBC concentrations at ABN ranged between 3 and 63 pg g^{-1} with a geometric mean of 20 pg g^{-1} which is considerably lower than rBC concentrations in modern snow at other sites (Roosevelt Island, West Antarctica, Law Dome and GV7) (Bisiaux et al., 2012; Caiazzo et al., 2017; Winton, Edwards, Delmonte, et al., 2016).

3.2. Stable Water Isotopes at ABN

The interpretation of stable water isotopes at ABN is described in Servettaz et al. (2020). Briefly, water stable isotopes measured in the ABN snow pit record atmospheric conditions during precipitation. Precipitation is distributed throughout the year but with a larger prevalence in winter. High snowfall events occur at ABN as a result of high-pressure anomalies that bring warm, moist air into the Antarctic continent. In particular, high snowfall events occurred in winter 2007, winter 2009, and winter 2011 (Figure 2d) associated with either (a) higher $\delta^{18}O$ values, a negative Southern Annular Mode (SAM), a higher Wilkes Land blocking index, and warm moist air masses from the Indian Ocean, or (b) higher than expected $\delta^{18}O$ values.

3.3. Enrichment Factor Analysis

The EFs of ABN snow samples are used to aid our interpretation of mineral dust versus other atmospheric sources. We note the limitations of using EFs for this purpose, such as whether the reference material (TDTi) is representative of mineral dust in the atmosphere compared to the crust (e.g., Shelley et al., 2015). The majority, that is, 90%, of EFs for TDFe and TDAl are low or moderately enriched, that is, EFs between 0.1 and 8 for TDFe and between 0.1 and 4 for TDAl. EFs in this range are similar to the UCC, suggesting that these trace metals have originated from other crustal material with a different composition from titanium (Duce et al., 1983). EFs for TDPb are >10 for 80% of the samples implying a significant non-crustal enrichment attributable to anthropogenic

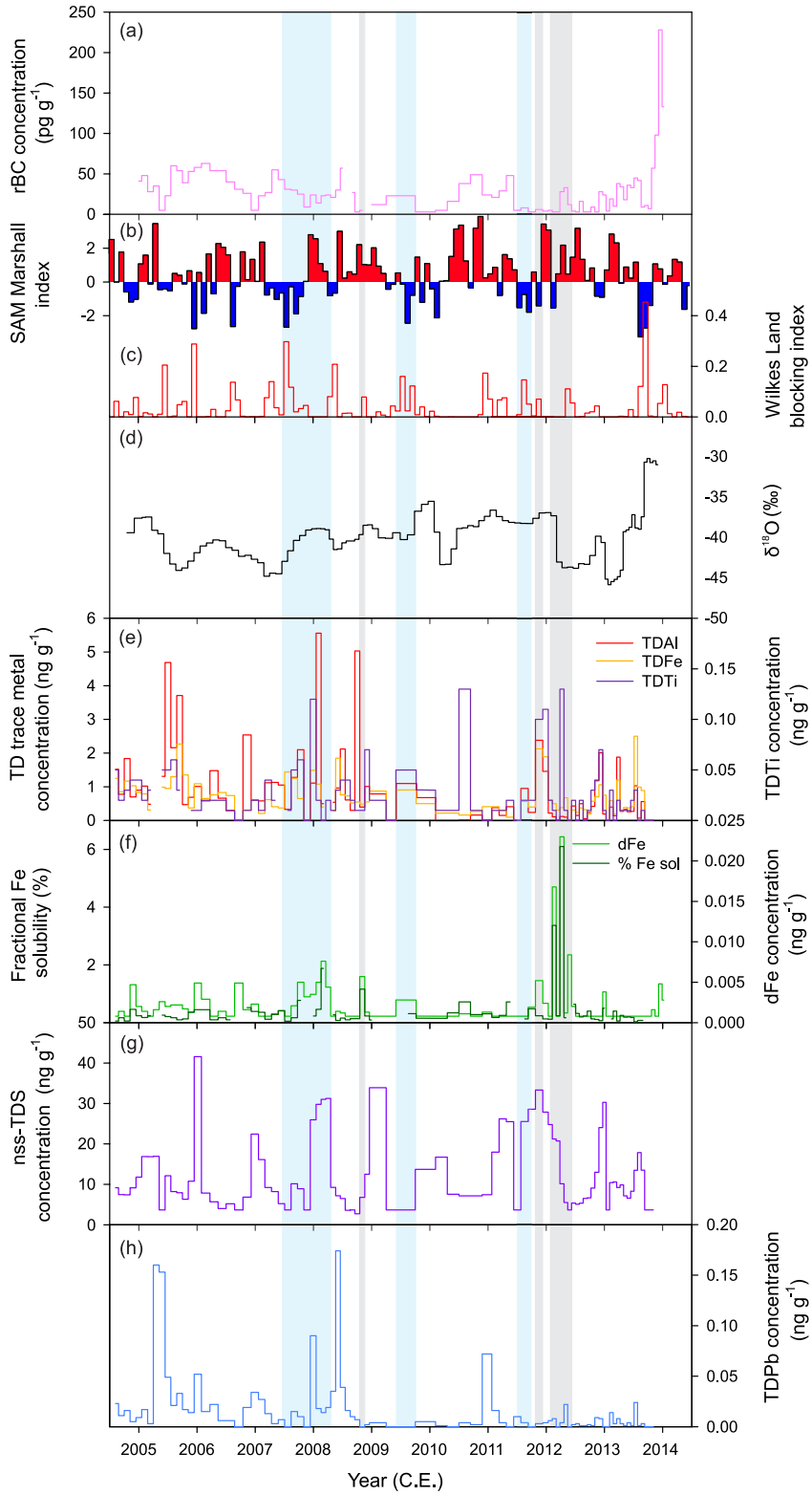
(a)
rBC concentration (pg g-1)
(b)
SAM Marshall index
(c)
Wilkes Land blocking index
(d)
δ18O (‰)
(e)
TDAl
TDFe
TDTi
TD trace metal concentration (ng g-1)
TDTi concentration (ng g-1)
(f)
dFe
% Fe sol
Fractional Fe solubility (%)
dFe concentration (ng g-1)
(g)
nss-TDS concentration (ng g-1)
(h)
TDPb concentration (ng g-1)
2005
2006
2007
2008
2009
2010
2011
2012
2013
2014
Year (C.E.)

Figure 2.

pollution consistent with the modern lead isotopic composition of Antarctic ice cores (McConnell et al., 2014). The low EFs for TDFe imply that biomass burning and pollution are relatively unimportant sources of atmospheric iron at the site.

3.4. Total Dissolvable Iron and Total Dissolvable Aluminum

TDAl and TDFe concentrations ranged from 0.1 ± 0.02 to 5.5 ± 0.3 ng g^{-1} and 0.1 ± 0.01 to 2.5 ± 0.2 ng g^{-1} respectively (Figure 2). Deposition of TDAl, TDFe and TDTi is episodic, rather than seasonal, with the largest deposition events occurring in winter 2005, winter 2007/summer 2007/2008, winter 2009, and spring 2011. A mineral dust source of TDFe is evident through (a) covariation of TDFe, TDAl, and TDTi concentrations in the snow pit (TDFe, TDAl: $r^2 = 0.23$, $P < 0.001$) (Figure 2e), (b) low fractional iron solubility (mean of 0.4 ± 0.8%) typical of mineral dust (see Section 3.5), and (c) low EFs indicative of UCC sources. Although the present-day geographic provenance of mineral dust is yet to be confirmed for the ABN site, modeling studies of airmass fetch regions suggested dust deposited in the Wilkes Land region could originate from mixed Southern Hemisphere sources including Australia and local Antarctic sources (F. Li et al., 2008; Neff & Bertler, 2015; Tatlhego et al., 2020). We note that the TDFe fluxes (see Section 3.6) are similar to other sites in Antarctica that are influenced by local dust, and thus cannot exclude a local dust source contributing to the TDFe fraction at ABN. In terms of local sources, new PSA such as Bunger Hills, proximal to the ABN site in East Antarctica, have been identified and the strontium (Sr) and neodymium (Nd) isotopic composition quantified in PSA samples (Delmonte et al., 2020). While we analyzed the Sr and Nd isotopic composition of dust from surface snow at ABN following Delmonte et al. (2020), the small dust sample with a low Nd concentration (~0.4 ng of Nd) provided only one $^{87}Sr/^{86}Sr$ value of 0.714335. While this value is similar to modern mixed dust sources in the Weddell Sea region and Princess Elizbeth Land in East Antarctica (Bory et al., 2010; Du et al., 2018), the interpretation of the dust provenance at ABN based on a single sample is inconclusive (Figure S4 and Table S3 in Supporting Information S1). Further work is required to identify the dust provenance of modern dust arriving at ABN.

3.5. Dissolved Iron and Fractional Iron Solubility

dFe concentrations were lower than TDFe concentrations and ranged between 0.001 ± 0.0003 and 0.02 ± 0.0001 ng g^{-1} (Figure 2). Fractional iron solubility ranged from 0.1% to 6% and parallels dFe concentration (Figure 2f). Fractional iron solubility has a positive linear relationship with dFe concentration ($r^2 = 0.89$, $P < 0.001$). Although the exposure blank concentrations of dFe are exceptionally low (Table S2 in Supporting Information S1), the dFe blank background is similar to some of the snow pit samples. Due to the extremely low dFe concentration of the snow pit samples, it is possible that the uncertainty on the blank concentrations could be responsible for some of the temporal variation. Nevertheless, there are periods in the ABN profile when fractional iron solubility at ABN exceeds the characteristic value for mineral dust of ~1%, suggesting other sources or processes influence fractional iron solubility during those periods (e.g., Ito et al., 2019; Sholkovitz et al., 2012). dFe deposition is episodic with the two largest deposition events occurring in summer 2007/2008 and late summer/autumn 2012 and smaller deposition events occurring in spring 2008, winter 2009, winter 2011, and spring 2011. These dFe deposition events are not consistently associated with deposition of mineral dust (TDAl and TDTi), TDFe, biomass burning (rBC), or lead pollution (TDPb concentration) but rather occur at same time as elevated $\delta^{18}O$ values, high precipitation, a negative SAM, and a high Wilkes Land blocking index. We discuss the possible reasons for the higher dFe deposition during such events in Section 3.7.

Figure 2. Variability in snow chemistry along the Aurora Basin North (ABN) snow pit profile (a) refractory black carbon (rBC) concentrations, (b) Wilkes Land blocking index (Servettaz et al., 2020), (c) Southern Annular Mode (SAM) Marshall monthly index (Marshall, 2003), (d) $\delta^{18}O$ values, (e) total dissolvable aluminum (TDAl) iron (TDFe) and titanium concentrations (TDTi), (f) dissolved iron (dFe) concentrations and fractional iron solubility (% Fe sol), (g) non-sea-salt-total dissolvable sulfur (nss-TDS) concentrations, and (h) total dissolvable lead (TDPb) concentrations. Periods of high snow accumulation, particularly negative SAM and high Wilkes Land blocking index, identified by Servettaz et al. (2020), are highlighted in blue with additional periods of negative SAM and high Wilkes Land blocking index highlighted in gray.

Table 1
Annual Dissolved Iron (dFe) and Total Dissolvable Iron (TDFe) Deposition Fluxes at Aurora Basin North

	TdFe flux (10^{-6} g m^{-2} yr^{-1})	dFe flux (10^{-6} g m^{-2} yr^{-1})
2005	116	0.2
2006	47	0.2
2007	62	0.2
2008	187	0.3
2009	10	0.02
2010	23	0.1
2011	45	0.1
2012	93	0.7
2013	94	0.2

3.6. Atmospheric Iron Fluxes

We calculate dFe and TDFe annual fluxes for the ABN record following the approach of Winton, Edwards, Delmonte, et al. (2016) and report the values in Table 1. Annual mean dFe and TDFe fluxes are $0.2 \pm 0.01 \times 10^{-6}$ g m^{-2} y^{-1} and $75 \pm 0.01 \times 10^{-6}$ g m^{-2} y^{-1} respectively. The only directly comparable study is the high-resolution snow pit from Roosevelt Island (Winton, Edwards, Delmonte, et al., 2016) that employed the same iron leaching protocol. The dFe and TDFe fluxes at ABN are lower than those at Roosevelt Island due to the higher elevation (2690 m vs. 550 m a.s.l) and longer distance inland (~500 vs. ~100 m) of ABN from the coast. In terms of TDFe variability between the sites, distally derived coarse mineral dust particles could reach coastal sites, such as Roosevelt Island, but are not transported further inland to higher elevation sites on the plateau. Furthermore, the coastal Roosevelt Island site is influenced by proximal dust sources from Marie Byrd Land contributing to the higher dFe and TDFe fluxes. In addition to Roosevelt Island, there are a few other sites in Antarctica where present day atmospheric iron fluxes have been estimated using similar iron leaching methods in Antarctic snow. Annual dFe and TDFe fluxes at Lambert Glacial Basin, East Antarctica, estimated from a snow pit spanning 2012–2017, are greater than ABN and remarkably similar to Roosevelt Island (dFe: 1.3×10^{-6} g m^{-2} y^{-1}; TDFe 140×10^{-6} g m^{-2} y^{-1}); the Lambert Glacial Basin site may also be influenced by local dust sources in East Antarctica (K. Liu et al., 2019). dFe and TDFe fluxes in surface snow along a transect from Zhongshan Station to Dome A in Princess Elizabeth Land, East Antarctica in austral summer 2017 were variable and ranged from 1.6 to 22 $\times 10^{-6}$ and 2.3 to 110 $\times 10^{-6}$ g m^{-2} y^{-1} respectively (Du et al., 2019). In a firn core, recovered 200 km from the coast along the Zhongshan Station to Dome A transect, dFe and TDFe fluxes averaged 21 and 61 $\times 10^{-6}$ g m^{-2} y^{-1} respectively between 1990 and 2017 and the variability was attributed to a mixture of mineral dust, volcanic and biomass burning sources of atmospheric iron (Du et al., 2020). Other estimates of TDFe in East Antarctic surface snow range from 28 $\times 10^{-6}$ g m^{-2} y^{-1} at Dumont D'urville to 60 $\times 10^{-6}$ g m^{-2} y^{-1} at Princess Elizabeth Land to 78 $\times 10^{-6}$ g m^{-2} y^{-1} at Prydz Bay to 87 $\times 10^{-6}$ g m^{-2} y^{-1} in the Ross Sea (Edwards & Sedwick, 2001). In summary, dFe fluxes at ABN are the lowest ever observed in Antarctica, while the TDFe fluxes are comparable to other sites in Antarctica.

3.7. Enhanced Soluble Iron Deposition by Atmospheric Processing

Here we investigate possible sources and processes to explain the episodic periods of elevated dFe deposition and fractional iron solubility in the ABN snow record. In terms of sources, mineral dust is generally considered the background source of dFe over Antarctica and the Southern Ocean (e.g., Vallelonga et al., 2013). Both the timing of dFe and TDFe/TDAl deposition is episodic with three periods of elevated dFe deposition coinciding with a spike in TDFe/TDAl deposition (winter 2007/summer 2007/2008, winter 2009, and spring 2011). However, not all spikes in TDFe deposition result in elevated dFe concentrations. Similar to other locations in the remote Southern Ocean, we suggest that mineral dust is the background source of dFe at ABN but as the dFe fluxes are the lowest observed over Antarctica, iron leached from long-range transported mineral dust reaching ABN is likely to supply relatively low inputs of bioavailable iron to the ocean. As with global datasets of fractional iron solubility (K. Liu et al., 2021; Sholkovitz et al., 2012; Winton, Edwards, Delmonte, et al., 2016), we observe a non-linear, inverse hyperbolic relationship between fractional iron solubility and TDFe in ABN and Roosevelt combined datasets suggesting additional sources and/or processes are acting to enhance the fractional iron solubility in Antarctica (Figure 3). At ABN, the majority of the fractional iron solubility values display the characteristic value for mineral dust of ~1% consistent with trace metal observations of a mineral dust source. While biomass burning is a suggested source of the higher fractional iron solubility at Roosevelt Island (Winton, Edwards, Delmonte, et al., 2016), the Antarctic compilation in Figure 3 highlights spatial differences in sources and processes influencing the atmospheric iron solubility. Recent global modeling of present day atmospheric soluble iron sources to oceanic waters estimates that sources of atmospheric dFe to Indian Ocean waters proximal to ABN are Australian and southern African dust and southern African combustion (Mahowald et al., 2018). We continue the discussion focusing on the periods of elevated dFe concentrations.

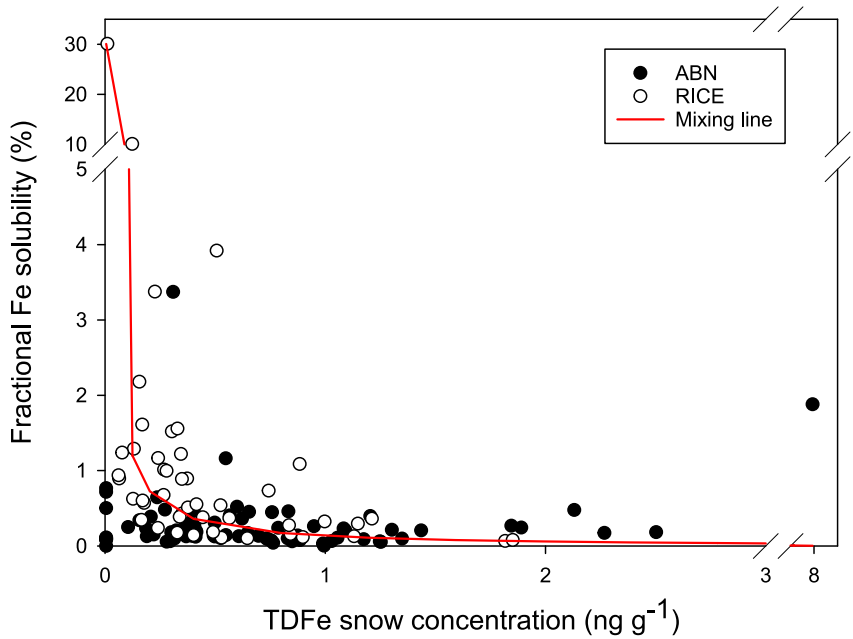

Figure 3. Inverse hyperbolic relationship between fractional iron solubility and total dissolvable iron (TDFe) in Antarctic snow pits from Aurora Basin North (ABN) and Roosevelt Island (RICE). The red line is a simple two endmember conservative mixing model between two source end members of (a) low fractional iron solubility and high TDFe concentrations (typical of mineral dust source) and (b) higher fractional iron solubility and low TDFe concentrations (typical of combustion source or atmospheric processing). RICE data source: Winton, Edwards, Delmonte, et al. (2016).

Biomass burning has been attributed to high dFe concentrations at a couple of coastal Antarctic sites and in long-range transported aerosol over the Southern Ocean by direct observation and modeling (Ito et al., 2019, 2020; Tang et al., 2021; Winton, Edwards, Delmonte, et al., 2016). Iron in freshly emitted biomass burning aerosol is relatively insoluble (Winton, Edwards, Bowie, et al., 2016) but biomass burning can indirectly impact atmospheric dFe during long-range transport through aggregation of iron and rBC particles (Ellis et al., 2015), oxalate modification in biomass burning plumes (Ito & Shi, 2016), and aging of combustion derived particles (Ito, 2015; Winton, Edwards, Bowie, et al., 2016). Although modeling studies show that fractional iron solubility and dFe fluxes over the ABN site lie in a plume directly downwind from southern African combustion sources (Ito et al., 2019; Ito & Shi, 2015), the extremely low rBC concentrations and non-coincident deposition timing of rBC and dFe suggests that biomass burning was an unimportant source of dFe during the study period.

Lead concentrations in modern Antarctic snow are derived from Southern Hemisphere anthropogenic activities. Furthermore, the non-crustal lead enrichment at ABN indicates anthropogenic pollution (see Section 3.3). We find no correlation between lead and dFe concentrations or fractional iron solubility at ABN. In summary, aside from the three deposition events where mineral dust contributed to the fractional iron solubility, we find that atmospheric iron sources such as mineral dust, biomass burning and lead pollution cannot explain the episodic high dFe concentrations and fractional iron solubility at ABN.

There is strong evidence that atmospheric processing can at least partly explain the enhanced fractional iron solubility in aerosols compared to fresh dust (Shi et al., 2012). In terms of atmospheric processes, oxalate modification, iron acidification and cloud processing are known to influence fractional iron solubility in long-range transported aerosol. Only trace concentrations of oxalate are found in air masses in lower latitudes over Antarctica and the Southern Ocean (Keywood, 2007). Although, little is known about the enhancement of fractional iron solubility in these pristine air masses, the concentrations of oxalate could be too low to influence fractional iron solubility of mineral dust. For example, no relationship was observed between oxalate and fractional iron solubility in a year long record of baseline air over the Southern Ocean at the Cape Grim Baseline Air Pollution Station (Winton et al., 2015).

Iron acidification occurs in the atmosphere by sulfur which is often the main acidic component of aerosols, and largely determines the acidity of fine particles. As such, studies show that the incorporation of sulfur dioxide (SO_2) into mineral dust plumes can subsequently acidify the iron contained in the mineral dust through SO_2 oxidation (Meskhidze et al., 2003; Zhuang et al., 1992). The spring 2010 deposition events of dFe coincided with elevated nss-TDS concentrations and higher TDFe/TDAl deposition in the snow pit and thus iron acidification by SO_2 could possibly explain the elevated dFe concentrations in snow. Previous observations of SO_2 acidification of iron bearing mineral dust occurred in highly polluted air masses over China with significantly higher concentrations of SO_2 in the atmosphere than over coastal East Antarctica where SO_2 concentrations are considerably lower and atmospheric sulfur is dominantly sourced from seasonal phytoplankton blooms (e.g., Jang et al., 2019). Given higher nss-TDS concentrations do not occur at all periods of enhanced dFe deposition, we suggest that SO_2 concentrations are too low to promote acidification of dFe in mineral dust in the East Antarctic region (Meskhidze et al., 2005). As acidity is relatively low in the atmosphere over Antarctica, we recommend future studies investigate the atmospheric processes that drive atmospheric iron solubility in remote, pristine air.

Cloud processing is where aerosols undergo multiple cycles of condensation and evaporation during their lifetime before being removed from the atmosphere through wet or dry deposition. These cycles induce large variations in the chemistry of the water around the aerosol particle which can increase the fractional iron solubility in those air masses (Desboeufs et al., 2001; Shi et al., 2009). Iron leaching and modeling experiments simulating the cycling of iron-bearing dust between wet aerosol and cloud droplets show that iron in mineral dust readily dissolves under acidic conditions that are relevant to wet aerosols. Whereas under higher pH conditions in clouds, iron dissolution is lower and dFe precipitates as poorly crystalline nanoparticles (Shi et al., 2015). As this process of evaporation and condensation is repeated, iron in both the nanoparticles and mineral dust continues to dissolve. The more cycles and longer duration of the acidic wet aerosol stage, the higher the solubility of atmospheric iron.

In addition, wet deposition by precipitation scavenging has been proposed to be more efficient than dry deposition in supplying dFe to the ocean. Modeling suggests that wet deposition of atmospheric iron over the open ocean in the Southern Ocean accounts for ~60% of total deposition and contains a greater fractional iron solubility than dry deposition of atmospheric iron (Gao et al., 2003). Observations in the subAntarctic Islands also show that wet deposition supplies more dFe to the ocean than dry deposition (Chance et al., 2015; Heimburger, Losno, & Triquet, 2013). dFe in rainwater collected from Kerguelen Island had an exceptionally high fractional iron solubility of 80% which was attributed to atmospheric iron undergoing several cloud and chemical processes during transport that significantly increased the iron solubility. Despite the emerging importance of wet deposition of atmospheric iron supply in the Southern Ocean and on a global scale, wet deposition of atmospheric iron is largely under quantified in the Southern Ocean as most observational studies have focused on dry deposition. Furthermore, iron input by precipitation scavenging may be related to episodes of high productivity in some oceanic regions (Gao et al., 2003).

We observe that the periods of enhanced dFe and fractional iron solubility in the ABN snow record occur during large snowfall events that are associated with higher $\delta^{18}O$ values (Figure 2). Servettaz et al. (2020) show that these high snowfall events are driven by synoptic, warm conditions that bring oceanic air masses to the ABN site. The start of the largest dFe event in 2012 is associated with high $\delta^{18}O$ values and negative SAM consistent with the other periods of enhanced dFe. While $\delta^{18}O$ values decrease during the 2012 event, a high Wilkes Land blocking index and warm temperatures modeled by Servettaz et al. (2020) indicate that the 2012 event was not associated with a sudden drop in temperature and that warm synoptic scale air masses delivered moisture to the site and increased dFe concentrations consistent with the other periods of enhanced dFe (Figures 2b and 2c). We note that our dFe measurements in snow reflect total (wet and dry) deposition of atmospheric iron. Although we cannot separate out the wet and dry deposition fluxes, based on previous estimates of wet deposition in the Southern Ocean we suggest that wet deposition of dFe during extreme precipitation events could be an important input of atmospheric iron to water surrounding coastal East Antarctica. Furthermore, iron dissolution can be promoted during multiple cycles of cloud processing, as discussed above. As dFe deposition appears unrelated to biomass burning, anthropogenic activities or mineral dust sources, cloud processing is the most plausible explanation for the elevated dFe deposition in high snowfall, synoptic conditions. This explanation is in agreement with another study of high dFe and fractional iron solubility in precipitation over the Southern Ocean (Heimburger, Losno, & Triquet, 2013). Therefore, we suggest that dFe deposition at intermediate elevation sites in East Antarctica is related to atmospheric transport and processing rather than atmospheric iron sources of biomass burning

and mineral dust which drive the variability of fractional iron solubility in coastal Antarctic locations (Winton, Edwards, Delmonte, et al., 2016). In summary, we suggest that enhanced dFe deposition in the ABN snow pit can be explained by air masses arriving at ABN containing long-range transported iron particles, that did not pass over major land masses and as a consequence underwent multiple cycles of cloud processes over the Southern Ocean which markedly increased the fractional iron solubility.

3.8. Implications for Ice Core Studies of Bioavailable Iron

While the focus of this study is on the modern variability of fractional iron solubility in pristine air masses, and we are not debating the importance of atmospheric iron inputs to the climate during glacial periods (e.g., Latimer et al., 2006; Martínez-García et al., 2014), we note the implications of this study on longer ice core records of atmospheric iron. The higher elevation ABN site highlights the complex interplay of sources and processes that modulate fractional iron solubility in pristine air masses that vary over time and space in Antarctica and the Southern Ocean. Rather than the total iron deposition, it is the bioavailable fraction of iron that is relevant for primary production. Fractional iron solubility, estimated from modern Antarctic snow, does not always parallel mineral dust, TDAl or TDFe concentrations. Rather, fractional iron solubility is episodic, and dFe concentrations reflect multiple sources and processes. The non-linear relationship between TDFe and fractional iron solubility is most apparent at ABN which is the furthest inland Antarctic site (Figure 3), where the correlation between dFe and TDAl or TDFe concentrations is the weakest. Due to this non-linear relationship in Antarctica, ice core proxies of mineral dust, TDFe or TDAl cannot simply be scaled up to estimate dFe inputs over time (e.g., Wolff et al., 2006). Previous atmospheric iron studies using Antarctic ice cores either have not measured the dFe fraction of iron (i.e., <0.2 μm), or they assumed a constant fractional iron solubility derived solely from dust and total iron sources (Edwards et al., 2006; Gaspari et al., 2006; Vallelonga et al., 2013). A few ice core methods have been developed for iron speciation (Burgay et al., 2021) or the continuous flow analysis (CFA) of iron concentrations in ice cores (Hiscock et al., 2013; Spolaor et al., 2013; Traversi et al., 2004) but each method employees a different leaching protocol that assesses a different pool of iron from mineral dust. Given our current understanding of the variability of fractional iron solubility, future studies should focus on direct measurements of dFe concentrations in ice cores. We recommend a standardized method for both dFe measurements in discrete snow samples and ice core dFe measurements using CFA. A standardized iron leaching method has been proposed by the aerosol iron community for more reliable intercomparison studies of atmospheric iron on different spatial and temporal scales (Perron et al., 2020).

With our new understanding of dFe variability in Antarctic snow, we carry out a simple thought experiment to estimate dFe deposition during the last glacial transition by applying the mixing model of the two end member components in Figure 3 to the European Project for Ice Coring in Antarctica (EPICA) Dome C ice core dust record (Lambert et al., 2008). We acknowledge a number of limitations and assumptions in this approach. As no direct TDFe concentrations are available for the Dome C core, we assume the total iron content in dust is 3.5 wt%. The calculated fractional iron solubility values therefore represent a lower limit. We also assume that the total iron content in dust is constant through time, although we acknowledge that the relationship between dust and total iron in Antarctic snow and ice is not always linear, especially for sites influenced by long-range transported dust. We find that fractional iron solubility is 20 times higher during the Holocene and drops off during the last glacial maximum (LGM; Figure S5 in Supporting Information S1). Based on our present day understanding of the mixing model, the increase in fractional iron solubility during the Holocene could be related to a shift from mineral dust to combustion atmospheric iron sources or increased atmospheric processing. Both higher dust concentrations (e.g., Delmonte et al., 2002) and more frequent Southern Hemispheric biomass burning (A. Chen et al., 2022) during the LGM than the Holocene have been observed. Alternatively, accumulation rates were higher during the Holocene which could lead to increased cloud processing and wet deposition. More evidence is required to support a shift in iron source and/or increased cloud processing as an explanation for the higher fractional iron solubility during the Holocene in the Dome C record. Interestingly, higher fractional iron solubility was observed during the Holocene compared to the LGM in the North Greenland Eemian Ice Drilling (NEEM) ice core attributed to changes in dust composition, grain size and other potential factors (Xiao et al., 2021). While in Antarctica, higher fractional iron solubility was observed during the LGM relative to the Holocene (Gaspari et al., 2006), although different iron leaching protocols pose limitations on the direct comparison of these studies. This highlights the large information gaps for past Antarctic iron deposition and solubility which requires future work.

While fractional iron solubility over the last glacial may have been minimal, atmospheric bioavailable iron deposition to the Southern Ocean was twice as high during the LGM, that is, the input of atmospheric dFe to phytoplankton was double than the present atmospheric input. New inputs of dFe from upwelling in the modern and paleo-Southern Ocean have been shown to be a key driver of primary production (Dulaiova et al., 2009; Jong et al., 2012; Marsay et al., 2014). Even if past natural iron-fertilization was low, future inputs of dFe could be higher, for example, combustion sources are predicted to rise over the next century (Lin et al., 2015; Pacyna & Pacyna, 2001; Scheiter et al., 2015), impacting the response of primary production to future ocean conditions (Boyd et al., 2015; Boyd et al., 2016; Henley et al., 2020; Morley et al., 2020). This simple thought experiment highlights that the relationship between dFe and mineral dust is complex and direct measurements of dFe are required to estimate atmospheric bioavailable iron inputs to the Southern Ocean over time.

4. Conclusions

A mean annual dFe deposition flux of $0.2 \pm 0.01 \times 10^{-6}$ g m^{-2} y^{-1} and a mean annual TDFe flux of $70 \pm 0.01 \times 10^{-6}$ g m^{-2} y^{-1} have been observed in modern Antarctic snow at the ABN site between 2004 and 2014. The dFe flux is the lowest observed for modern Antarctic snow, while the TDFe is comparable to other Antarctic sites. These fluxes to the Antarctic snow represent total atmospheric iron deposition (wet and dry). We find that wet deposition of dFe during high snowfall events is the dominant deposition mode at intermediate sites in East Antarctica (i.e., 2690 m a.s.l and 550 km from the coast). While TDFe at ABN originates from mineral dust, as does background dFe deposition, episodic deposition of elevated dFe is unrelated to atmospheric iron sources of mineral dust or biomass burning. rBC concentrations at ABN are relatively low, averaging ~20 pg g^{-1} between 2005 and 2014 with rBC deposition occurring at different times of the year. This study shows that the five periods of enhanced dFe deposition in the ABN snow pit record are associated with warm synoptic conditions (high snowfall and high $\delta^{18}O$ values), and we interpret this to reflect cloud processing of iron bearing mineral dust that increases the solubility of atmospheric iron during long-range transport from Southern Hemispheric dust sources. Therefore, dFe at ABN reflects atmospheric processing and transport rather than sources. This is the first study in modern Antarctic snow highlighting the importance of atmospheric processing, aerosol aging and transport on dFe deposition. While mineral dust likely supplies the background atmospheric dFe inputs to Southern Ocean and Antarctic waters, episodic deposition of atmospheric iron from other sources, for example, mineral dust, biomass burning and volcanic emissions, are observed at coastal Antarctic sites. At ABN, fractional iron solubility ranged from 0.1% to 6%. Even at the extremely remote, higher elevation Antarctic site of ABN, the relationship between fractional iron solubility and TDFe concentration is not linear, as observed on a global scale. We caution against using mineral dust or TDFe in ice cores as a proxy for bioavailable iron supply to the Southern Ocean over time. Overall, this study highlights a complex interplay of sources and processes that drive the solubility of atmospheric iron in pristine air masses over the Southern Ocean. Given the importance of wet deposition at higher elevation Antarctic sites and at other subAntarctic Island sites, and the scarcity of such measurements in the region, we recommend future studies quantify wet deposition of dFe in the Southern Ocean.

Conflict of Interest

The authors declare no conflicts of interest relevant to this study.

Data Availability Statement

The data set for the ABN trace element and rBC concentrations are available through the Australian Antarctic Data Centre (Winton et al., 2022) available at https://doi.org/10.26179/5efec17c04747 and supporting data are also included as tables in Supporting Information S1 files.

Acknowledgments
This work was supported by the Australian Antarctic Division (AAS 4075), and the Australian Government's Cooperative Research Centres Programme through the Antarctic Climate and Ecosystems Cooperative Research Centre (ACE CRC). The authors would like to thank the Australian Antarctic Division and Casey Station personnel for logistical support. Thank you to the ABN field team for assisting in the collection of samples from Aurora Basin North, in particular thanks to Olivia Maselli, Chris Plummer, and Mana Inoue for snow pit digging and sampling in less than favorable weather conditions. Thanks to Jason Roberts for measuring the geographic coordinates of the snow pit site. Thank you to Ross Edwards for insightful discussions. Technical support was provided by Ross Edwards, Jarrad Radon and Gwyn Huges at the TRACE Facility, Curtin University. The authors acknowledge the Australian Antarctic Division for providing the Aurora Basin North Automatic Weather Station data http://aws.cdaso.cloud.edu.au/ last accessed 15 December 2021. Access to HR-ICP-MS instrumentation at Curtin University was facilitated through ARC LIEF funding (LE130100029). Isotopic analyses for dust provenance characterization were carried out at the Swedish Museum of Natural History and were supported by the Department of Geosciences, Swedish Museum of Natural History. V.H.L.W. was supported by an Australian Postgraduate Award and Curtin Research Scholarship, and by a Rutherford Foundation Postdoctoral Fellowship administrated by the Royal Society Te Apārangi. Open access publishing facilitated by Curtin University, as part of the Wiley - Curtin University agreement via the Council of Australian University Librarians.

References

Ayers, G. P. (2001). Influence of local soil dust on composition of aerosol samples at Cape Grim Baseline Atmospheric Program (Australia) 1997-98, Baseline report (pp. 50–56).

Becagli, S., Marchese, C., Caiazzo, L., Ciardini, V., Lazzara, L., Mori, G., et al. (2022). Biogenic aerosol in central East Antarctic Plateau as a proxy for the ocean-atmosphere interaction in the Southern Ocean. *Science of the Total Environment*, *810*, 151285. https://doi.org/10.1016/j.scitotenv.2021.151285

Bisiaux, M., Edwards, R., McConnell, J., Curran, M., Van Ommen, T., Smith, A., et al. (2012). Changes in black carbon deposition to Antarctica from two high-resolution ice core records, 1850–2000 AD. *Atmospheric Chemistry and Physics*, *12*(9), 4107–4115. https://doi.org/10.5194/acp-12-4107-2012

Bodhaine, B. A. (1995). Aerosol absorption measurements at Barrow, Mauna Loa and the South pole. *Journal of Geophysical Research*, *100*(D5), 8967–8975. https://doi.org/10.1029/95jd00513

Bory, A., Wolff, E., Mulvaney, R., Jagoutz, E., Wegner, A., Ruth, U., & Elderfield, H. (2010). Multiple sources supply Eolian mineral dust to the Atlantic sector of coastal Antarctica: Evidence from recent snow layers at the top of Berkner Island ice sheet. *Earth and Planetary Science Letters*, *291*(1–4), 138–148. https://doi.org/10.1016/j.epsl.2010.01.006

Bowie, A. R., Lannuzel, D., Remenyi, T. A., Wagener, T., Lam, P. J., Boyd, P. W., et al. (2009). Biogeochemical iron budgets of the Southern Ocean South of Australia: Decoupling of iron and nutrient cycles in the sub-Antarctic zone by the summertime supply. *Global Biogeochemical Cycles*, *23*(4), GB4034. https://doi.org/10.1029/2009gb003500

Boyd, P. W., Claustre, H., Levy, M., Siegel, D. A., & Weber, T. (2019). Multi-faceted particle pumps drive carbon sequestration in the ocean. *Nature*, *568*(7752), 327–335. https://doi.org/10.1038/s41586-019-1098-2

Boyd, P. W., Dillingham, P., McGraw, C., Armstrong, E., Cornwall, C. E., Feng, Y.-Y., et al. (2016). Physiological responses of a Southern Ocean diatom to complex future ocean conditions. *Nature Climate Change*, *6*(2), 207–213. https://doi.org/10.1038/nclimate2811

Boyd, P. W., Lennartz, S. T., Glover, D. M., & Doney, S. C. (2015). Biological ramifications of climate-change-mediated oceanic multi-stressors. *Nature Climate Change*, *5*(1), 71–79. https://doi.org/10.1038/nclimate2441

Boyd, P. W., Watson, A. J., Law, C. S., Abraham, E. R., Trull, T., Murdoch, R., et al. (2000). A mesoscale phytoplankton bloom in the polar Southern Ocean stimulated by iron fertilization. *Nature*, *407*(6805), 695–702. https://doi.org/10.1038/35037500

Burgay, F., Barbaro, E., Cappelletti, D., Turetta, C., Gallet, J.-C., Isaksson, E., et al. (2021). First discrete iron (II) records from Dome C (Antarctica) and the Holtedahlfonna glacier (Svalbard). *Chemosphere*, *267*, 129335. https://doi.org/10.1016/j.chemosphere.2020.129335

Caiazzo, L., Baccolo, G., Barbante, C., Becagli, S., Bertò, M., Ciardini, V., et al. (2017). Prominent features in isotopic, chemical and dust stratigraphies from coastal East Antarctic ice sheet (Eastern Wilkes Land). *Chemosphere*, *176*, 273–287. https://doi.org/10.1016/j.chemosphere.2017.02.115

Chance, R., Jickells, T. D., & Baker, A. R. (2015). Atmospheric trace metal concentrations, solubility and deposition fluxes in remote marine air over the south-east Atlantic. *Marine Chemistry*, *176*, 273–287. https://doi.org/10.1016/j.marchem.2015.06.028

Chen, A., Yang, L., Kang, H., Gao, Y., & Xie, Z. (2022). Southern hemisphere fire history since the late glacial, reconstructed from an Antarctic sediment core. *Quaternary Science Reviews*, *276*, 107300. https://doi.org/10.1016/j.quascirev.2021.107300

Chen, Y., & Siefert, R. L. (2004). Seasonal and spatial distributions and dry deposition fluxes of atmospheric total and labile iron over the tropical and subtropical North Atlantic Ocean. *Journal of Geophysical Research*, *109*(D9), D09305. https://doi.org/10.1029/2003jd003958

Conway, T., Wolff, E., Röthlisberger, R., Mulvaney, R., & Elderfield, H. (2015). Constraints on soluble aerosol iron flux to the Southern Ocean at the last glacial maximum. *Nature Communications*, *6*(7850), 1–9. https://doi.org/10.1038/ncomms8850

Curran, M. A., & Palmer, A. S. (2001). Suppressed ion chromatography methods for the routine determination of ultra low level anions and cations in ice cores. *Journal of Chromatography A*, *919*(1), 107–113. https://doi.org/10.1016/s0021-9673(01)00790-7

Delmonte, B., Petit, J. R., & Maggi, V. (2002). Glacial to Holocene implications of the new 27000-year dust record from the EPICA Dome C (East Antarctica) ice core. *Climate Dynamics*, *18*(8), 647–660. https://doi.org/10.1007/s00382-001-0193-9

Delmonte, B., Winton, H., Baroni, M., Baccolo, G., Hansson, M., Andersson, P., et al. (2020). Holocene dust in East Antarctica: Provenance and variability in time and space. *The Holocene*, *30*(4), 546–558. https://doi.org/10.1177/0959683619875188

Deppeler, S. L., & Davidson, A. T. (2017). Southern Ocean phytoplankton in a changing climate. *Frontiers in Marine Science*, *4*(40). https://doi.org/10.3389/fmars.2017.00040

Desboeufs, K., Losno, R., & Colin, J.-L. (2001). Factors influencing aerosol solubility during cloud processes. *Atmospheric Environment*, *35*(20), 3529–3537. https://doi.org/10.1016/s1352-2310(00)00472-6

Dinniman, M. S., St-Laurent, P., Arrigo, K. R., Hofmann, E. E., & van Dijken, G. L. (2020). Analysis of iron sources in Antarctic continental shelf waters. *Journal of Geophysical Research: Oceans*, *125*(5), e2019JC015736. https://doi.org/10.1029/2019jc015736

Du, Z., Xiao, C., Ding, M., & Li, C. (2018). Identification of multiple natural and anthropogenic sources of dust in snow from Zhongshan Station to Dome A, East Antarctica. *Journal of Glaciology*, *64*(248), 855–865. https://doi.org/10.1017/jog.2018.72

Du, Z., Xiao, C., Handley, M. J., Mayewski, P. A., Li, C., Liu, S., et al. (2019). Fe variation characteristics and sources in snow samples along a traverse from Zhongshan Station to Dome A, East Antarctica. *Science of the Total Environment*, *675*, 380–389. https://doi.org/10.1016/j.scitotenv.2019.04.139

Du, Z., Xiao, C., Mayewski, P. A., Handley, M. J., Li, C., Ding, M., et al. (2020). The iron records and its sources during 1990-2017 from the Lambert Glacial Basin shallow ice core, East Antarctica. *Chemosphere*, 126399.

Duce, R., Arimoto, R., Ray, B., Unni, C., & Harder, P. (1983). Atmospheric trace elements at Enewetak Atoll: 1. Concentrations, sources, and temporal variability. *Journal of Geophysical Research*, *88*(C9), 5321–5342. https://doi.org/10.1029/jc088ic09p05321

Dulaiova, H., Ardelan, M., Henderson, P. B., & Charette, M. A. (2009). Shelf-derived iron inputs drive biological productivity in the southern Drake Passage. *Global Biogeochemical Cycles*, *23*(4). https://doi.org/10.1029/2008gb003406

Duprat, L., Corkill, M., Genovese, C., Townsend, A., Moreau, S., Meiners, K., & Lannuzel, D. (2020). Nutrient distribution in East Antarctic summer sea ice: A potential iron contribution from glacial basal melt. *Journal of Geophysical Research: Oceans*, *125*(12), e2020JC016130. https://doi.org/10.1029/2020jc016130

Edwards, R., & Sedwick, P. (2001). Iron in East Antarctic snow: Implications for atmospheric iron deposition and algal production in Antarctic waters. *Geophysical Research Letters*, *28*(20), 3907–3910. https://doi.org/10.1029/2001gl012867

Edwards, R., Sedwick, P., Morgan, V., & Boutron, C. (2006). Iron in ice cores from Law Dome: A record of atmospheric iron deposition for maritime east Antarctica during the Holocene and last glacial maximum. *Geochemistry, Geophysics, Geosystems*, *7*(12), Q12Q01. https://doi.org/10.1029/2006GC001307

Eichler, A., Gramlich, G., Kellerhals, T., Tobler, L., & Schwikowski, M. (2015). Pb pollution from leaded gasoline in South America in the context of a 2000-year metallurgical history. https://doi.org/10.1126/sciadv.1400196

Ellis, A., Edwards, R., Saunders, M., Chakrabarty, R., Subramanian, R., van Riessen, A., et al. (2015). Characterizing black carbon in rain and ice cores using coupled tangential flow filtration and transmission electron microscopy.

Gao, Y., Fan, S.-M., & Sarmiento, J. L. (2003). Aeolian iron input to the ocean through precipitation scavenging: A modeling perspective and its implication for natural iron fertilization in the ocean. *Journal of Geophysical Research*, *108*(D7), 4221. https://doi.org/10.1029/2002jd002420

Gao, Y., Xu, G., Zhan, J., Zhang, J., Li, W., Lin, Q., et al. (2013). Spatial and particle size distributions of atmospheric dissolvable iron in aerosols and its input to the Southern Ocean and coastal East Antarctica. *Journal of Geophysical Research: Atmospheres*, *118*(22), 634–612. https://doi.org/10.1002/2013jd020367

Gao, Y., Yu, S., Sherrell, R. M., Fan, S., Bu, K., & Anderson, J. R. (2020). Particle-size distributions and solubility of aerosol iron over the Antarctic peninsula during austral summer. *Journal of Geophysical Research: Atmospheres*, *125*(11), e2019JD032082. https://doi.org/10.1029/2019jd032082

Gaspari, V., Barbante, C., Cozzi, G., Cescon, P., Boutron, C. F., Gabrielli, P., et al. (2006). Atmospheric iron fluxes over the last deglaciation: Climatic implications. *Geophysical Research Letters*, *33*(3), L03704. https://doi.org/10.1029/2005gl024352

Hand, J. L., Mahowald, N. M., Chen, Y., Siefert, R. L., Luo, C., Subramaniam, A., & Fung, I. (2004). Estimates of atmospheric-processed soluble iron from observations and a global mineral aerosol model: Biogeochemical implications. *Journal of Geophysical Research*, *109*(D17), D17205. https://doi.org/10.1029/2004jd004574

Heimburger, A., Losno, R., & Triquet, S. (2013). Solubility of iron and other trace elements in rainwater collected on the Kerguelen Islands (South Indian Ocean). *Biogeosciences*, *10*(10), 6617–6628. https://doi.org/10.5194/bg-10-6617-2013

Heimburger, A., Losno, R., Triquet, S., Dulac, F., & Mahowald, N. (2012). Direct measurements of atmospheric iron, cobalt, and aluminum-derived dust deposition at Kerguelen Islands. *Global Biogeochemical Cycles*, *26*(4), 2012GB004301. https://doi.org/10.1029/2012gb004301

Heimburger, A., Losno, R., Triquet, S., & Nguyen, E. (2013). Atmospheric deposition fluxes of 26 elements over the southern Indian Ocean: Time series on Kerguelen and Crozet islands. *Global Biogeochemical Cycles*, *27*(2), 440–449. https://doi.org/10.1002/gbc.20043

Henley, S. F., Cavan, E. L., Fawcett, S. E., Kerr, R., Monteiro, T., Sherrell, R. M., et al. (2020). Changing biogeochemistry of the Southern Ocean and its ecosystem implications. *Frontiers in Marine Science*, *7*, 581. https://doi.org/10.3389/fmars.2020.00581

Hiscock, W. T., Fischer, H., Bigler, M., Gfeller, G., Leuenberger, D., & Mini, O. (2013). Continuous flow analysis of labile iron in ice-cores. *Environmental Science & Technology*, *47*(9), 4416–4425. https://doi.org/10.1021/es3047087

Ito, A. (2015). Atmospheric processing of combustion aerosols as a source of bioavailable iron. *Environmental Science and Technology Letters*, *2*(3), 70–75. https://doi.org/10.1021/acs.estlett.5b00007

Ito, A., Myriokefalitakis, S., Kanakidou, M., Mahowald, N. M., Scanza, R. A., Hamilton, D. S., et al. (2019). Pyrogenic iron: The missing link to high iron solubility in aerosols. *Science Advances*, *5*(5), eaau7671. https://doi.org/10.1126/sciadv.aau7671

Ito, A., Perron, M. M., Proemse, B. C., Strzelec, M., Gault-Ringold, M., Boyd, P. W., & Bowie, A. R. (2020). Evaluation of aerosol iron solubility over Australian coastal regions based on inverse modeling: Implications of bushfires on bioaccessible iron concentrations in the southern hemisphere. *Progress in Earth and Planetary Science*, *7*(1), 1–17. https://doi.org/10.1186/s40645-020-00357-9

Ito, A., & Shi, Z. (2015). Delivery of anthropogenic bioavailable iron from mineral dust and combustion aerosols to the ocean. *Atmospheric Chemistry and Physics Discussions*, *15*(16), 23051–23088.

Ito, A., & Shi, Z. (2016). Delivery of anthropogenic bioavailable iron from mineral dust and combustion aerosols to the ocean. *Atmospheric Chemistry and Physics*, *16*(1), 85–99. https://doi.org/10.5194/acp-16-85-2016

Jang, E., Park, K.-T., Yoon, Y. J., Kim, T.-W., Hong, S.-B., Becagli, S., et al. (2019). New particle formation events observed at the King Sejong Station, Antarctic Peninsula–Part 2: Link with the oceanic biological activities. *Atmospheric Chemistry and Physics*, *19*(11), 7595–7608. https://doi.org/10.5194/acp-19-7595-2019

Jong, J., Schoemann, V., Lannuzel, D., Croot, P., Baar, H., & Tison, J. L. (2012). Natural iron fertilization of the Atlantic sector of the Southern Ocean by continental shelf sources of the Antarctic Peninsula. *Journal of Geophysical Research*, *117*(G1). https://doi.org/10.1029/2011jg001679

Keywood, M. D. (2007). Aerosol composition at Cape Grim: An evaluation of PM10 sampling program and baseline event switches. In J. M. Cainey, N. Derek, & P. B. Krummel (Eds.), *Baseline atmospheric program Australia 2005-2006. 2005-2006*, (pp. 31–36). Australian Bureau of Meteorology and CSIRO marine and atmospheric Research.

Lambert, F., Delmonte, B., Petit, J. R., Bigler, M., Kaufmann, P. R., Hutterli, M. A., et al. (2008). Dust-climate couplings over the past 800,000 years from the EPICA Dome C ice core. *Nature*, *452*(7187), 616–619. https://doi.org/10.1038/nature06763

Lannuzel, D., Vancoppenolle, M., Van der Merwe, P., De Jong, J., Meiners, K. M., Grotti, M., et al. (2016). Iron in sea ice: Review and new insights. *Elementa: Science of the Anthropocene*, *4*, https://doi.org/10.12952/journal.elementa.000130

Latimer, J. C., Filippelli, G. M., Hendy, I. L., Gleason, J. D., & Blum, J. D. (2006). Glacial-interglacial terrigenous provenance in the southeastern Atlantic Ocean: The importance of deep-water sources and surface currents. *Geology*, *34*(7), 545–548. https://doi.org/10.1130/g22252.1

Li, F., Ginoux, P., & Ramaswamy, V. (2008). Distribution, transport, and deposition of mineral dust in the Southern Ocean and Antarctica: Contribution of major sources. *Journal of Geophysical Research*, *113*(D10), D10207. https://doi.org/10.1029/2007jd009190

Li, W., Xu, L., Liu, X., Zhang, J., Lin, Y., Yao, X., et al. (2017). Air pollution–aerosol interactions produce more bioavailable iron for ocean ecosystems. *Science Advances*, *3*(3), e1601749. https://doi.org/10.1126/sciadv.1601749

Lin, Y. C., Chen, J. P., Ho, T. Y., & Tsai, I. (2015). Atmospheric iron deposition in the northwestern Pacific Ocean and its adjacent marginal seas: The importance of coal burning. *Global Biogeochemical Cycles*, *29*(2), 138–159. https://doi.org/10.1002/2013gb004795

Liu, K., Hou, S., Wu, S., Pang, H., Zhang, W., Song, J., et al. (2021). The atmospheric iron variations during 1950–2016 recorded in snow at Dome Argus, East Antarctica. *Atmospheric Research*, *248*, 105263. https://doi.org/10.1016/j.atmosres.2020.105263

Liu, K., Hou, S., Wu, S., Zhang, W., Zou, X., Pang, H., et al. (2019). Dissolved iron concentration in the recent snow of the Lambert Glacial Basin, Antarctica. *Atmospheric Environment*, *196*, 44–52. https://doi.org/10.1016/j.atmosenv.2018.10.011

Liu, T., Mickley, L. J., Marlier, M. E., DeFries, R. S., Khan, M. F., Latif, M. T., & Karambelas, A. (2020). Diagnosing spatial biases and uncertainties in global fire emissions inventories: Indonesia as regional case study. *Remote Sensing of Environment*, *237*, 111557. https://doi.org/10.1016/j.rse.2019.111557

Mahowald, N., Hamilton, D., Mackey, K., Moore, J., Baker, A., Scanza, R., & Zhang, Y. (2018). Aerosol trace metal leaching and impacts on marine microorganisms. *Nature Communications*, *176*(1), 273–287. https://doi.org/10.1038/s41467-018-04970-7

Marsay, C., Sedwick, P. N., Dinniman, M., Barrett, P., Mack, S., & McGillicuddy, D. J. (2014). Estimating the benthic efflux of dissolved iron on the Ross Sea continental shelf. *Geophysical Research Letters*, *41*(21), 7576–7583. https://doi.org/10.1002/2014gl061684

Marshall, G. J. (2003). Trends in the southern Annular mode from observations and reanalyses. *Journal of Climate*, *16*(24), 4134–4143. https://doi.org/10.1175/1520-0442(2003)016<4134:titsam>2.0.co;2

Martínez-García, A., Sigman, D. M., Ren, H., Anderson, R. F., Straub, M., Hodell, D. A., et al. (2014). Iron fertilization of the subantarctic ocean during the last ice age. *Science*, *343*(6177), 1347–1350. https://doi.org/10.1126/science.1246848

McConnell, J. R., Maselli, O. J., Sigl, M., Vallelonga, P., Neumann, T., Anschütz, H., et al. (2014). Antarctic-wide array of high-resolution ice core records reveals pervasive lead pollution began in 1889 and persists today. *Scientific Reports*, *4*(1), 5848. https://doi.org/10.1038/srep05848

Meskhidze, N., Chameides, W., Nenes, A., & Chen, G. (2003). Iron mobilization in mineral dust: Can anthropogenic SO2 emissions affect ocean productivity? *Geophysical Research Letters*, *30*(21), 2085. https://doi.org/10.1029/2003gl018035

Meskhidze, N., Chameides, W. L., & Nenes, A. (2005). Dust and pollution: A recipe for enhanced ocean fertilization? *Journal of Geophysical Research*, *110*(D3), D03301. https://doi.org/10.1029/2004jd005082

Miller, W. L., King, D. W., Lin, J., & Kester, D. R. (1995). Photochemical redox cycling of iron in coastal seawater. *Marine Chemistry*, *50*(1–4), 63–77. https://doi.org/10.1016/0304-4203(95)00027-o

Morley, S. A., Abele, D., Barnes, D. K. A., Cardenas, C. A., Cotte, C., Gutt, J., et al. (2020). Global drivers on Southern Ocean ecosystems: Changing physical Environments and anthropogenic pressures in an Earth system. *Frontiers in Marine Science*, *7*(1097). https://doi.org/10.3389/fmars.2020.547188

Neff, P. D., & Bertler, N. A. (2015). Trajectory modeling of modern dust transport to the Southern Ocean and Antarctica. *Journal of Geophysical Research: Atmospheres*, *176*(18), 273–287. https://doi.org/10.1002/2015jd023304

Pacyna, J. M., & Pacyna, E. G. (2001). An assessment of global and regional emissions of trace metals to the atmosphere from anthropogenic sources worldwide. *Environmental Reviews*, *9*(4), 269–298. https://doi.org/10.1139/a01-012

Paris, R., Desboeufs, K., & Journet, E. (2011). Variability of dust iron solubility in atmospheric waters: Investigation of the role of oxalate organic complexation. *Atmospheric Environment*, *45*(36), 6510–6517. https://doi.org/10.1016/j.atmosenv.2011.08.068

Perron, M. M., Strzelec, M., Gault-Ringold, M., Proemse, B. C., Boyd, P. W., & Bowie, A. R. (2020). Assessment of leaching protocols to determine the solubility of trace metals in aerosols. *Talanta*, *208*, 120377. https://doi.org/10.1016/j.talanta.2019.120377

Pinkerton, M. H., Boyd, P. W., Deppeler, S., Hayward, A., Höfer, J., & Moreau, S. (2021). Evidence for the impact of climate change on primary producers in the Southern Ocean. *Frontiers in Ecology and Evolution*, *9*, 592027. https://doi.org/10.3389/fevo.2021.592027

Plummer, C. T., Curran, M. A., van Ommen, T. D., Rasmussen, S. O., Moy, A. D., Vance, T. R., et al. (2012). An independently dated 2000-yr volcanic record from Law Dome, East Antarctica, including a new perspective on the dating of the 1450s CE eruption of Kuwae, Vanuatu. *Climate of the Past*, *8*(6), 1929–1940. https://doi.org/10.5194/cp-8-1929-2012

Reimann, C., & Caritat, P. D. (2000). Intrinsic flaws of element enrichment factors (EFs) in environmental geochemistry. *Environmental Science & Technology*, *34*(24), 5084–5091. https://doi.org/10.1021/es001339o

Rivaro, P., Ardini, F., Vivado, D., Cabella, R., Castagno, P., Mangoni, O., & Falco, P. (2020). Potential sources of particulate iron in surface and deep waters of the Terra Nova Bay (Ross Sea, Antarctica). *Water*, *12*(12), 3517. https://doi.org/10.3390/w12123517

Rose, J., Feng, Y., DiTullio, G. R., Dunbar, R. B., Hare, C., Lee, P., et al. (2009). Synergistic effects of iron and temperature on Antarctic phytoplankton and microzooplankton assemblages. *Biogeosciences*, *6*(12), 3131–3147. https://doi.org/10.5194/bg-6-3131-2009

Salmon, E., Hofmann, E. E., Dinniman, M. S., & Smith, W. O., Jr. (2020). Evaluation of iron sources in the Ross Sea. *Journal of Marine Systems*, *212*, 103429. https://doi.org/10.1016/j.jmarsys.2020.103429

Scheiter, S., Higgins, S. I., Beringer, J., & Hutley, L. B. (2015). Climate change and long-term fire management impacts on Australian Savannas. *New Phytologist*, *205*(3), 1211–1226. https://doi.org/10.1111/nph.13130

Servettaz, A. P., Orsi, A. J., Curran, M. A., Moy, A. D., Landais, A., Agosta, C., et al. (2020). Snowfall and water stable isotope variability in East Antarctica controlled by warm synoptic events. *Journal of Geophysical Research: Atmospheres*, *125*(17), e2020JD032863. https://doi.org/10.1029/2020jd032863

Shelley, R. U., Morton, P. L., & Landing, W. M. (2015). Elemental ratios and enrichment factors in aerosols from the US-GEOTRACES North Atlantic transects. *Deep Sea Research Part II: Topical Studies in Oceanography*, *116*, 262–272. https://doi.org/10.1016/j.dsr2.2014.12.005

Shi, Z., Krom, M. D., Bonneville, S., Baker, A. R., Jickells, T. D., & Benning, L. G. (2009). Formation of iron nanoparticles and increase in iron reactivity in mineral dust during simulated cloud processing. *Environmental Science & Technology*, *43*(17), 6592–6596. https://doi.org/10.1021/es901294g

Shi, Z., Krom, M. D., Bonneville, S., & Benning, L. G. (2015). Atmospheric processing outside clouds increases soluble iron in mineral dust. *Environmental Science & Technology*, *49*(3), 1472–1477. https://doi.org/10.1021/es504623x

Shi, Z., Krom, M. D., Jickells, T. D., Bonneville, S., Carslaw, K. S., Mihalopoulos, N., et al. (2012). Impacts on iron solubility in the mineral dust by processes in the source region and the atmosphere: A review. *Aeolian Research*, *5*, 21–42. https://doi.org/10.1016/j.aeolia.2012.03.001

Sholkovitz, E. R., Sedwick, P. N., Church, T. M., Baker, A. R., & Powell, C. F. (2012). Fractional solubility of aerosol iron: Synthesis of a global-scale data set. *Geochimica et Cosmochimica Acta*, *89*, 173–189. https://doi.org/10.1016/j.gca.2012.04.022

Spolaor, A., Vallelonga, P., Gabrieli, J., Roman, M., & Barbante, C. (2013). Continuous flow analysis method for determination of soluble iron and aluminium in ice cores. *Analytical and Bioanalytical Chemistry*, *405*(2–3), 767–774. https://doi.org/10.1007/s00216-012-6166-5

Sterle, K. M., McConnell, J. R., Dozier, J., Edwards, R., & Flanner, M. (2013). Retention and radiative forcing of black carbon in eastern Sierra Nevada snow. *The Cryosphere*, *7*(1), 365–374. https://doi.org/10.5194/tc-7-365-2013

Tagliabue, A., Bowie, A. R., Boyd, P. W., Buck, K. N., Johnson, K. S., & Saito, M. A. (2017). The integral role of iron in ocean biogeochemistry. *Nature*, *543*(7643), 51–59. https://doi.org/10.1038/nature21058

Tang, W., Llort, J., Weis, J., Perron, M. M., Basart, S., Li, Z., et al. (2021). Widespread phytoplankton blooms triggered by 2019–2020 Australian wildfires. *Nature*, *597*(7876), 370–375. https://doi.org/10.1038/s41586-021-03805-8

Tatlhego, M., Bhattachan, A., Okin, G. S., & D'Odorico, P. (2020). Mapping areas of the Southern Ocean where productivity likely depends on dust-delivered iron. *Journal of Geophysical Research: Atmospheres*, *125*(3), e2019JD030926. https://doi.org/10.1029/2019jd030926

Traversi, R., Barbante, C., Gaspari, V., Fattori, I., Largiuni, O., Magaldi, L., & Udisti, R. (2004). Aluminium and iron record for the last 28 kyr derived from the Antarctic EDC96 ice core using new CFA methods. *Annals of Glaciology*, *39*, 300–306. https://doi.org/10.3189/172756404781814438

Vallelonga, P., Barbante, C., Cozzi, G., Gabrieli, J., Schüpbach, S., Spolaor, A., & Turetta, C. (2013). Iron fluxes to Talos Dome, Antarctica, over the past 200 kyr. *Climate of the Past*, *9*(2), 597–604. https://doi.org/10.5194/cp-9-597-2013

Weber, T. (2020). Southern Ocean upwelling and the marine iron cycle. *Geophysical Research Letters*, *47*(20), e2020GL090737. https://doi.org/10.1029/2020gl090737

Wedepohl, K. H. (1995). The composition of the continental crust. *Geochimica et Cosmochimica Acta*, *59*(7), 1217–1232. https://doi.org/10.1016/0016-7037(95)00038-2

Winton, V., Dunbar, G., Atkins, C., Bertler, N., Delmonte, B., Andersson, P., et al. (2016). The origin of lithogenic sediment in the south-western Ross Sea and implications for iron fertilization. *Antarctic Science*, *28*(4), 250–260. https://doi.org/10.1017/s095410201600002x

Winton, V. H. L., Bowie, A. R., Edwards, R., Keywood, M., Townsend, A. T., van der Merwe, P., & Bollhöfer, A. (2015). Fractional iron solubility of atmospheric iron inputs to the Southern Ocean. *Marine Chemistry*, *177*(1), 20–32. https://doi.org/10.1016/j.marchem.2015.06.006

Winton, V. H. L., Dunbar, G. B., Bertler, N. A. N., Millet, M. A., Delmonte, B., Atkins, C. B., et al. (2014). The contribution of aeolian sand and dust to iron fertilization of phytoplankton blooms in Southwestern Ross Sea, Antarctica. *Global Biogeochemical Cycles*, *28*(4), 2013GB004574. https://doi.org/10.1002/2013GB004574

Winton, V. H. L., & Edwards, R. (2022). Trace metal and back carbon concentrations in the Aurora Basin North 13/14 snow pit. [Dataset]. Australian Antarctic Data Centre. https://doi.org/10.26179/5efec17c04747

Winton, V. H. L., Edwards, R., Bowie, A. R., Keywood, M., Williams, A. G., Chambers, S. D., et al. (2016). Dry season aerosol iron solubility in tropical northern Australia. *Atmospheric Chemistry and Physics*, *16*(19), 12829–12848. https://doi.org/10.5194/acp-16-12829-2016

Winton, V. H. L., Edwards, R., Delmonte, B., Ellis, A., Andersson, P. S., Bowie, A., et al. (2016). Multiple sources of soluble atmospheric iron to Antarctic waters. *Global Biogeochemical Cycles*, *30*(3), 421–437. https://doi.org/10.1002/2015GB005265

Wolff, E. W., & Cachier, H. (1998). Concentrations and seasonal cycle of black carbon in aerosol at a coastal Antarctic station. *Journal of Geophysical Research*, *103*(D9), 11033–11041. https://doi.org/10.1029/97jd01363

Wolff, E. W., Fischer, H., Fundel, F., Ruth, U., Twarloh, B., Littot, G. C., et al. (2006). Southern Ocean sea-ice extent, productivity and iron flux over the past eight glacial cycles. *Nature*, *440*(7083), 491–496. https://doi.org/10.1038/nature04614

Xiao, C., Du, Z., Handley, M. J., Mayewski, P. A., Cao, J., Schüpbach, S., et al. (2021). Iron in the NEEM ice core relative to Asian loess records over the last glacial–interglacial cycle. *National Science Review*, *8*(7), nwaa144. https://doi.org/10.1093/nsr/nwaa144

Zhuang, G., Yi, Z., Duce, R. A., & Brown, P. R. (1992). Link between iron and sulphur cycles suggested by detection of Fe (n) in remote marine aerosols. *Nature*, *355*(6360), 537–539. https://doi.org/10.1038/355537a0

References From the Supporting Information

Blakowski, M. A., Aciego, S. M., Delmonte, B., Baroni, C., Salvatore, M. C., & Sims, K. W. W. (2016). A Sr-Nd-Hf isotope characterization of dust source areas in Victoria Land and the McMurdo Sound Sector of Antarctica. *Quaternary Science Reviews*, *141*, 26–37. https://doi.org/10.1016/j.quascirev.2016.03.023

Delmonte, B., Baroni, C., Andersson, P. S., Schoberg, H., Hansson, M., Aciego, S., et al. (2010). Aeolian dust in the Talos Dome ice core (East Antarctica, Pacific/Ross Sea sector): Victoria Land versus remote sources over the last two climate cycles. *Journal of Quaternary Science*, *25*(8), 1327–1337. https://doi.org/10.1002/jqs.1418

Delmonte, B., Basile-Doelsch, I., Petit, J. R., Maggi, V., Revel-Rolland, M., Michard, A., et al. (2004). Comparing the Epica and Vostok dust records during the last 220,000 years: Stratigraphical correlation and provenance in glacial periods. *Earth-Science Reviews*, *66*(1–2), 63–87. https://doi.org/10.1016/j.earscirev.2003.10.004

Draxler, R. R., & Rolph, G. D. (2003). Hybrid single-particle Lagrangian integrated trajectory (HYSPLIT), model (Vol. *176*).

Gili, S., Gaiero, D. M., Goldstein, S. L., Chemale, F., Jr., Jweda, J., Kaplan, M. R., et al. (2017). Glacial/interglacial changes of Southern Hemisphere wind circulation from the geochemistry of South American dust. *Earth and Planetary Science Letters*, *469*, 98–109. https://doi.org/10.1016/j.epsl.2017.04.007